January 2010

Gel-carbon nanotube materials: the relationship between nanotube network connectivity and conductivity

Naratip Songmee

Pisith Singjai

Marc in het Panhuis
University of Wollongong, panhuis@uow.edu.au

Recommended Citation

Gel-carbon nanotube materials: the relationship between nanotube network connectivity and conductivity

Abstract

The electrical resistance of carbon nanotube networks (NNs) prepared from combinations of gellan gum, xanthan gum, Triton X-100, SWNT and MWNT is reported. It is demonstrated that the NN conductivity can be obtained by analysing the resistance of two overlapping NN as a function of their overlap distance. Unexpectedly, the connectivity between two overlapping NN was found to scale with the electrical conductivity over 4 orders of magnitude. Insights into the dependence of inter-NN contact on applied pressure were obtained.

Keywords

connectivity, gel, network, between, relationship, materials, nanotube, conductivity, carbon

Disciplines

Life Sciences | Physical Sciences and Mathematics | Social and Behavioral Sciences

Publication Details

Gel–carbon nanotube materials: the relationship between nanotube network connectivity and conductivity

Naratip Songmee,[ab] Pisith Singjai[b] and Marc in het Panhuis[*a]

The electrical resistance of carbon nanotube networks (NNs) prepared from combinations of gellan gum, xanthan gum, Triton X-100, SWNT and MWNT is reported. It is demonstrated that the NN conductivity can be obtained by analysing the resistance of two overlapping NN as a function of their overlap distance. Unexpectedly, the connectivity between two overlapping NN was found to scale with the electrical conductivity over 4 orders of magnitude. Insights into the dependence of inter-NN contact on applied pressure were obtained.

Introduction

It is well-known that the electrical properties of individual carbon nanotubes (CNTs) are superior to those of carbon nanotube networks (NNs).[1–6] The reported conductivity values for individual CNTs are in excess of 8×10^6 S m^{-1}.[2,3] In contrast, typical conductivity values for NN are below 10^4 S m^{-1}, although this can be improved through chemical treatment.[5,6] Single CNT device applications dictate fabrication of individual single-walled carbon nanotubes (SWNTs) with specific electrical properties. For example, field effect transistor devices require semi-conducting SWNT, whereas interconnects require metallic SWNT.[7,8] Reliable fabrication of individual SWNT remains an issue due to the inability to control chirality and therefore electronic properties during synthesis. In contrast, NNs can be reproducibly fabricated using various methods involving vacuum filtration, evaporative casting, inkjet printing, spraying and spin coating of CNT dispersions as well as direct growth methods.[9–17] The advantage of a NN is that the influence of an individual CNT's chirality is minimised, with the network containing both semi-conducting and metallic pathways. Hence, NN can serve as either semi-conducting channels or conducting sheets.[16,18–20] These electrical properties combined with their flexible nature make NN ideal for a number of potential applications such as solar cells, displays, touch screens, sensors and electronic paper.[15,17]

The dispersability of CNTs in most common solvents is rather limited, but it is well-known that this can be improved through the use of dispersants such as surfactants and polymers.[4] Recently, it has been demonstrated that gel forming biopolymers such as gum arabic, gellan gum (GG), xanthan gum (XG) and the carrageenans are efficient CNT stabilisers.[21–26]

GG and XG are linear anionic polysaccharides produced in high yields by the *Sphingomonas elodea* and *Xanthomonas campestris* bacteria, respectively.[27–29] They are US FDA and European Union (E415 and E418) approved for food usage, and have found wide application as multi-functional gelling, stabilising and suspending agents. In addition, these polymers are also in use as encapsulating agents and active ingredients in drug delivery applications and are emerging as a material for the construction of three-dimensional scaffolds for tissue engineering applications.[30,31]

It has been demonstrated that GG and XG can form transparent CNT composite gels that can be used in the preparation of NN through inkjet printing and evaporative casting.[21,26] Percolation studies revealed that a MWNT concentration of 1.3% by weight is required to achieve an electrically conducting NN in a gellan gum hydrogel.[23] The resulting nanotube networks consist of pathways dominated by intra-CNT and CNT–polymer–CNT junctions, with the latter junction acting as a tunnelling barrier.[21,23] It has been shown that for NN the level of graphitisation, type of nanotubes (SWNT and MWNT) and network morphology are important factors determining NN conductivity.[32] However, the most important factor determining the transport through a nanotube network is the resistance of the NN junctions.[15,32]

In this paper, we investigate the electrical resistance of NN prepared by vacuum filtration and evaporative casting of gellan gum-SWNT, gellan gum-MWNT, xanthan gum-SWNT, xanthan gum-MWNT and Triton X-100-SWNT dispersions. We demonstrate that the NN conductivity can be obtained by analysing the resistance of two overlapping NN as a function of their overlap distance (under constant applied pressure). Unexpectedly, the connectivity between two overlapping NN was found to scale with the electrical conductivity over 4 orders of magnitude. Moreover, we show that insights into the dependence of inter-NN contact on applied pressure can be obtained through resistance measurements as a function of applied pressure on two overlapping NN (at a constant overlap distance).

Experimental

Dispersion preparation

Purified single-walled carbon nanotubes (SWNTs) produced by the high-pressure decomposition of carbon monoxide (HiPCO) process and multi-walled carbon nanotubes (MWNTs) produced by catalytic chemical vapour deposition (CVD) were obtained

[a]Soft Materials Group, School of Chemistry, University of Wollongong, Wollongong, Australia. E-mail: panhuis@uow.edu.au; Fax: +61 24221 4287; Tel: +61 24221 3155
[b]Nanomaterials Research Unit, Department of Physics and Materials Science, Faculty of Science, Chiang Mai University, Chiang Mai, 50200, Thailand

from Carbon Nanotechnologies, Inc. (lot # P0348) and Nanocyl S.A. (lot # NFL60). Gellan gum (GG, low acyl, molecular weight, $M_w \approx 2$ to 3×10^5 Da, lot # 7C9228A) and xanthan gum (XG, $M_w \approx 1 \times 10^6$ Da, lot # 9D4608K) were gifts from CP Kelco. Triton X-100 (TX, $M_w \approx 625$ Da) was obtained from Sigma Aldrich. All materials were used as received.

Solutions of GG (1.0% w/v) and XG (0.5% and 1.0% w/v) in Milli-Q water (18 MΩ cm) were prepared by adding 100 mg (GG) and 50 mg (XG) to 10 mL of water and stirring for 2 hours at 70 °C, respectively. Solutions of TX (1.0% w/v) were prepared by dissolving TX in water at 21 °C.

Homogeneous CNT dispersions were prepared by the probe sonication process in a Branson 450 (400 W, Ultrasonics Corp.) digital sonicator horn for up to 24 min in a pulse mode (0.5 s on/off). Different amounts and types of CNTs were dispersed in various solutions as shown in Table 1. For example, "XG05-MW005" indicates a typical dispersion used for evaporative casting prepared by dispersing MWNT (0.05% w/v) in XG solution (20 mL, 0.5% w/v). Whereas "TX1-SW00375" indicates a typical dispersion used for vacuum filtration prepared by dispersing SWNT (0.1% w/v) in a TX solution (30 mL, 1.0% w/v). The resulting dispersion is then combined with 50 mL TX solution (1.0% w/v) and sonicated for 3 min in an ultrasonic bath (Unisonics). The resulting SWNT concentration in the dispersion is 0.0375% w/v.

Preparation of NN by evaporative casting

Five NNs (E1–E5, Table 1) were prepared by evaporative casting of CNT dispersions onto plastic substrates. 5 mL of dispersion were injected into the base of a cylindrical plastic container (diameter ≈ 5.5 cm) and dried at 21 °C for 24 hours. The films were then peeled off the substrate to yield uniform free-standing NN.

Table 1 Summary of conductivity and contact resistance values for carbon nanotube networks (NNs). Samples E1–E5 and B1–B3 indicate NN prepared using evaporative casting and vacuum filtration of dispersions, respectively. The naming of the dispersions is as follows: dispersant concentration–CNT concentration, *e.g.* "GG1-MW005" indicates a dispersion with gellan gum (GG) and MWNT (MW) concentrations of 1.0% w/v and 0.05% w/v, respectively. XG, TX and SW indicate xanthan gum, Triton X-100 and SWNT, respectively. The bulk conductivity (σ) and electrode–NN contact resistance values are determined using fitted date to eqn (2). The overall conductivity (σ_{ov}) and NN1–NN2 contact resistance (R_{12}) values were determined using fitted date to eqn (2) and (5). R_{12} is obtained from measurements using two of the same NNs overlapping with each other, *e.g.* NN1 = E1 and NN2 = E1. The only exception is E2–B3, which indicates data obtained NN1 = E2 and NN2 = B3

NN sample	Dispersion	σ/S m^{-1}	R_C/kΩ	σ_{ov}/S m^{-1}	R_{12}/kΩ
E1	GG1-MW005	20.0 ± 3.0	0.956	24.7 ± 4.5	22.1
E2	GG1-MW01	110 ± 10	1.4	87 ± 10	2.78
E3	XG1-MW01	2.07 ± 0.14	10.8	2.65 ± 0.18	43.9
E4	XG05-MW005	1.46 ± 0.11	1.15	4.0 ± 0.3	90.4
E5	XG05-SW005	0.96 ± 0.05	3.82	0.93 ± 0.05	564
B1	XG03-SW003	357 ± 29	0.250	621 ± 50	0.055
B2	GG1-SW00375	386 ± 40	0.286	200 ± 10	0.599
B3	TX1-SW00375	10 155 ± 476	0.251	15 152 ± 172	0.006
E2 + B3	—	—	—	36 ± 18	11.3

Preparation of NN by vacuum filtration

Three NNs (B1–B3, Table 1) were prepared by vacuum filtration of GG-SWNT, XG-SWNT and TX-SWNT dispersions through a 0.45 μm nylon membrane filter (Micro Filtration Systems) housed in an Aldrich glass filtration unit, and using a Vacuubrand CVC2 pump that typically operated between 30 and 40 mbar. The tops of the filtration units were covered with film to prevent evaporative losses during the filtration process, which typically took approximately 1 day. Once a dispersion had been filtered, the resulting NN (buckypaper) was washed with 250 mL of Milli-Q water followed by 10 mL of methanol (99.8%, Merck) whilst still in the filtration unit. After washing, the damp buckypaper was placed between absorbent paper sheets and allowed to dry further overnight. The dry buckypaper (diameter 3.7 cm) was then carefully peeled away from the underlying commercial membrane filter.

Characterisation techniques

Current (I)–voltage (V) characteristics were determined using an in-house designed environmental chamber interfaced with a waveform generator (Agilent 33220A) and a digital multimeter (Agilent 34410A) under controlled ambient conditions in air (21 °C, 45% relative humidity, RH).

For resistance measurements as a function of length, NNs were cut into strips of 0.5 cm in width and lengths of up to 3.0 cm and contacted with conducting silver paint and copper electrodes. I–V measurements were made as a function of NN length, by cutting the end off the strip, contacting with silver/copper and re-measuring the I–V characteristics and repeating. Film thicknesses were determined using a Mitutoyo digital micrometre.

Resistance measurements for two overlapping NN were carried out by cutting two NN into strips (width = 0.5 cm, length = 2.0 cm), followed by contacting on one side with silver paint and copper electrodes. The NN samples were then overlapped at a particular distance (under a constant applied pressure to the overlap area) and measuring the I–V characteristics. The resistance was measured as a function of the overlap distance, by changing the overlap distance, applying constant pressure to the overlap area and re-measuring the I–V characteristics and repeating. Film thicknesses were determined using a Mitutoyo digital micrometre.

Resistance measurements as a function of pressure (2000 to 140 000 N m^{-2}) were carried out on two overlapping NN at a constant overlap distance of 1.0 cm. I–V measurements were made as a function of pressure, by changing the pressure, re-measuring the I–V characteristics and repeating.

Scanning electron microscopy (SEM) images were obtained using a JEOL field emission-SEM (JSM-6335F).

Results and discussion

Resistance as a function of NN length

Eight carbon nanotube networks (NNs, Table 1) were formed by evaporative casting and vacuum filtration of GG-SWNT, GG-MWNT, XG-SWNT, XG-MWNT and TX-SWNT dispersions.

The current–voltage (I–V) characteristics of these NNs were investigated under controlled ambient conditions (21 °C, 45%

RH). All films exhibited linear I–V characteristics, which indicate Ohmic behaviour. These were used to calculate the electrical resistances. However, the resulting values represent the total resistance (R_T) which is equal to the sum of the NN resistance (R_S) and the electrode–NN contact resistance (R_C):

$$R_T = R_S + R_C. \qquad (1)$$

Previously, it has been shown that R_T scales linearly with sample length (l) for a wide variety of NN according to:[20,21]

$$R_T = \frac{l}{\sigma A} + R_C, \qquad (2)$$

where σ and A are the bulk conductivity and cross-sectional area, respectively. Typical straight line fits for two of our NN prepared using vacuum filtration and evaporative casting of CNT dispersions are shown in Fig. 1. The slope is used to calculate the DC conductivity, while the intercept with the y-axis yields the R_C value.

Table 1 shows that the conductivity values of buckypaper NN (B1–B3) are higher compared to those for NN prepared by evaporative casting. For example, the σ and R_C values of a xanthan gum buckypaper (B1) are 357 ± 29 S m^{-1} and 250 Ω, respectively. Although this is a low conductivity value for buckypapers,[6,20] it is in agreement with our recently reported values for buckypapers prepared using biopolymer dispersants.[22] In comparison, the conductivity of a xanthan gum-SWNT NN prepared by evaporative casting (E5) is almost 3 orders of magnitude smaller (0.96 ± 0.05 S cm^{-1}), while the contact resistance is more than an order of magnitude larger (3820 Ω).

The likeness in CNT loading fraction (9.1%) of NN E2–E5 allows a comparison of the electrical properties between biopolymer dispersants and CNTs. Using XG as dispersant for MWNT results in NN exhibiting a lower conductivity compared to using GG as dispersant, i.e. $\sigma = 2.07 \pm 0.14$ S m^{-1} (E3) vs. $\sigma = 110 \pm 10$ S m^{-1} (E2). A comparison between NN E4 and E5 shows that at the same CNT loading fraction NN with SWNT exhibit a lower conductivity compared to the MWNT NN.
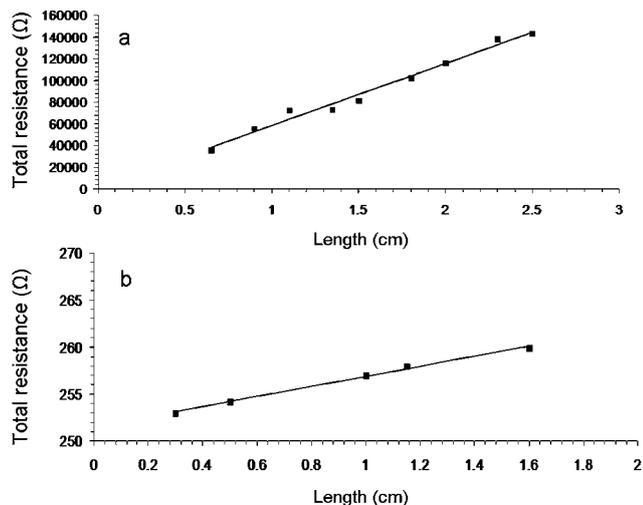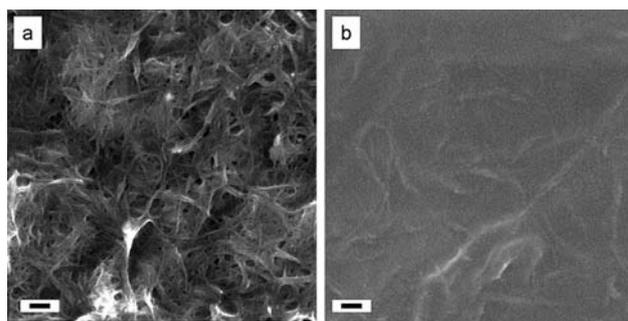
Fig. 2 Scanning electron microscopy images of carbon nanotube networks B1 (a) and E5 (b) prepared by vacuum filtration and evaporative casting of XG-HiPco SWNT dispersions, respectively. Scale bars indicate 100 nm.

The similarity in R_C values observed for the three buckypapers B1–B3 indicates that the minimum obtained NN–electrode contact resistance of our experimental setup is approximately 250 Ω. The larger R_C values exhibited for the samples prepared by evaporative casting suggest that something is impeding connectivity between NN and electrodes. Fig. 2 shows that there is a significant difference in surface morphology between the two types of NNs. The difference in morphology can be attributed to the extensive washing procedure during vacuum filtration, which removes dispersant. The NN is clearly visible in the buckypaper sample, but almost entirely covered by biopolymer in the sample prepared by evaporative casting.

We have previously shown that biopolymers such as gellan gum act as a tunnelling barrier blocking transport in electrical pathways.[21,23] Tunneling barriers can affect both sample and contact resistance. It is well-known that the pathways through a NN are dominated by inter-nanotube junctions, while in recent work we demonstrated that for biopolymers such as gellan gum there are also additional pathways dominated by nanotube–biopolymer–nanotube junctions.[21] There we reported that under ambient conditions these additional pathways are blocked due to GG acting as a tunnelling barrier. Therefore it can be assumed that there are two types of pathways between NN and electrode: (1) CNT–electrode and (2) CNT–biopolymer–electrode connections. It is suggested that the higher R_C values observed for samples prepared by evaporative casting originate from the biopolymer acting as insulating layer, and hence impede the connectivity between NN and electrode. This indicates that both the conductivity and contact resistance are influenced by the NN

Fig. 1 Resistance versus length for typical carbon nanotube networks E4 (a) and B3 (b) prepared by evaporative casting and vacuum filtration of XG-MWNT and TX-HiPco SWNT dispersions, respectively. The straight lines are fits to eqn (2).

Table 2 Pressure coefficients (t) and NN1–NN2 contact resistance in the absence of applied pressure (R_{120}) for selected carbon nanotube networks (NNs). E1, E2, E4, E5, B1 and B3 refer to NN compositions as listed in Table 1

NN sample	R_{120}/kΩ	t
E1	90.5	−0.3036
E2	12.5	−0.2077
E4	231	−0.1403
E5	942	−0.0324
B1	0.207	−0.0966
B3	0.0144	−0.0988

connectivity. However, the data in Table 2 show that connectivity cannot be estimated through a comparison of σ and R_C values. The R_C values of NN B1 and B3 are similar which suggest that the connectivity between NN and electrodes is not impeded, but this is contradicted by their σ values which vary by almost two orders of magnitude.

Resistance of overlapping NN

A more detailed analysis of NN connectivity can be obtained by evaluating the resistance of two overlapping NN (lengths l_1 and l_2, thickness t_1 and t_2, and width w) which are contacted on one side with electrodes, and overlap by a distance (l_{ov}) as shown in Scheme 1.

Using eqn (1) it can be shown that the total electrical resistance of this arrangement is as follows:

$$R_T = R_1 + R_2 + R_{12} + R_{C1} + R_{C2}, \quad (3)$$

where R_1, R_2, R_{12}, R_{C1} and R_{C2} are the resistances of NN1 and 2, the NN1–NN2 contact resistance, and the NN–electrode contact resistances of NN1 and NN2, respectively. Realising that electron transport through the sample is in the length direction, while that through the overlap region is in the thickness direction we obtain:

$$R_T = \frac{l_1 - l_{ov}}{\sigma_{ov} t_1 w} + \frac{t_1}{\sigma_{ov} l_{ov} w} + \frac{t_2}{\sigma_{ov} l_{ov} w} + \frac{l_2 - l_{ov}}{\sigma_{ov} t_2 w} + R_{12} + R_{C1} + R_{C2}, \quad (4)$$

with NN width w, and overall conductivity σ_{ov}. The only variable in this equation is the overlap distance, assuming a constant pressure is applied to the overlap area. The unknowns in this equation are the overall conductivity and the NN1–NN2 contact resistance. All other terms can be either measured directly (i.e. length, width and thickness) or obtained by fitting the R_T versus l data to eqn (2) as described above. Resistance measurements were made on two overlapping samples (under constant applied pressure) as a function of l_{ov} as shown in Fig. 3. The resistance scaled linearly with overlap parameter,

$$O_P = \frac{l_1 - l_{ov}}{t_1} + \frac{t_1}{l_{ov}} + \frac{t_2}{l_{ov}} + \frac{l_2 - l_{ov}}{t_2}$$

as described by

$$R_T = \frac{1}{\sigma_{ov} w} O_P + R_{12} + R_{C1} + R_{C2}. \quad (5)$$

The overlap parameter is a dimensionless number, and is indicative of the overlapped area. The slope of the straight line
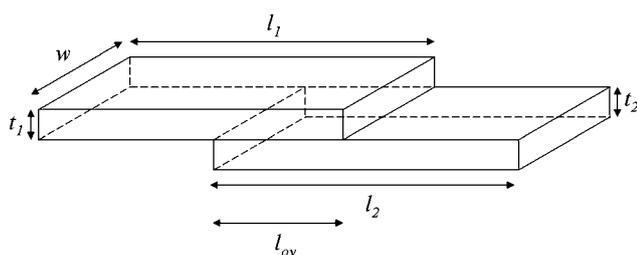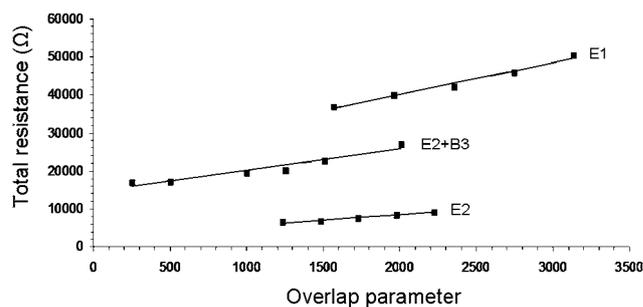

Fig. 3 Resistance as a function of the overlap parameter for typical carbon nanotube networks (NN) under constant applied pressure. E1, E2 and E2 + B3 refer to NN compositions as listed in Table 1. The straight lines are fits to eqn (5).

fits to eqn (5) is used to calculate σ_{ov}, while the intercept with the y-axis yields $R_{12} + R_{C1} + R_{C2}$. The latter values, R_{C1} and R_{C2}, can be obtained from the R_C values obtained from the R_T vs. l measurements discussed in the previous section. Note: R_C (NN1) $= 2R_{C1}$ and R_C (NN2) $= 2R_{C2}$, as R_C is the contact resistance of a NN contacted on both sides with electrodes, whereas R_{C1} and R_{C2} refer to the values of two overlapping NN contacted on one side.

Table 1 shows that there is good agreement between the conductivity values calculated using eqn (2) and (5). This demonstrates that the use of overlapping NNs is a viable method for evaluating the electrical conductivity of conducting samples. In addition, our method can be used to calculate the NN1–NN2 contact resistance as well as to analyse the effects of varying pressure on the resistance (discussed in the next section).

In the previous section we showed that, although the R_C values exhibited for samples B1–B3 were similar, their conductivity values varied over 2 orders of magnitude. The difference in the NN1–NN2 contact resistance values of B1 ($R_{12} = 55\ \Omega$), B2 ($R_{12} = 599\ \Omega$) and B3 ($R_{12} = 6\ \Omega$) can be used to explain the difference in the observed conductivity values. R_{12} is a measure of inter-NN pathways, i.e. the connectivity between NN1 and NN2. This parameter may also be seen as a measure of the pathways within a NN. After all, the highest conductivity will be observed for those NNs with the lowest CNT–CNT junction resistance. It is clear from Table 1 that the magnitude of the
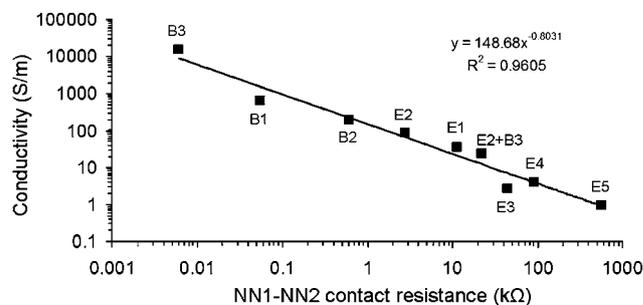

Fig. 4 Conductivity as a function of NN1–NN2 contact resistance (R_{12}) for overlapping carbon nanotube networks under constant applied pressure. E1–E5, B1–B3 and E2 + B3 refer to NN compositions as listed in Table 1. The line is a fit to eqn (6).

Scheme 1

conductivity is directly related to the magnitude of the NN1–NN2 contact resistance. For example, the σ and R_{12} value of E5 are 4 orders of magnitude lower compared to those of B3.

Fig. 4 shows the conductivity *versus* NN1–NN2 contact resistance under constant applied pressure, which scales according to

$$\sigma = \sigma_C R_{12}^m, \tag{6}$$

where σ_C is the conductivity at $R_{12} = 1 \text{ k}\Omega$ and m the power law exponent. The conductivity of NN scales over 4 orders of magnitude with $m = -0.8031$ and clearly demonstrates that NN–NN contact resistance is inversely proportional to conductivity. This is an exciting and unexpected result. Some dependency was expected (as mentioned above), but only for those NNs fabricated with the same type of dispersant, CNTs and processing method. Our results appear to suggest that m is an inherent NN parameter independent of the three dispersants (gellan gum, xanthan gum and Triton X-100), two types of CNTs (HiPCO SWNT and CVD MWNT), and two different fabrication methods (evaporative casting and vacuum filtration) used to form these NNs.

Resistance as a function of applied pressure

All resistance measurements in the previous section were carried out under a constant applied pressure to the overlap area, while varying the overlap parameter. This allowed us to demonstrate that m is an inherent NN parameter. However, m does not give us information about the dependence of inter-NN contact resistance on pressure in the overlap region. A way to measure this is to evaluate the effect of pressure on the NN1–NN2 contact resistance by varying the applied pressure on the overlap area, while keeping the overlap parameter O_P constant as shown in Fig. 5. As the pressure is applied only to the overlap area, and not to the NN1 electrode and the NN2 electrode contacts, eqn (5) can be employed to convert R_T values into R_{12} values (Fig. 5). The results can be fitted to
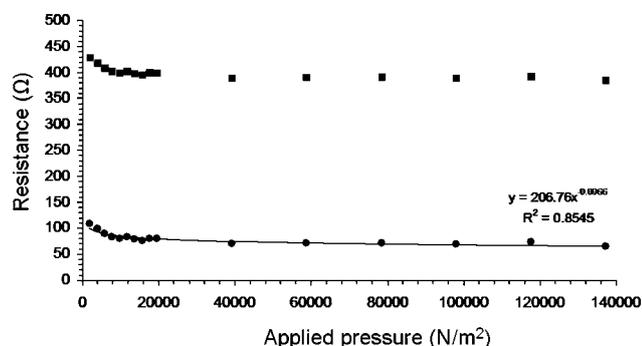
$$R_{12} = R_{120} P^t, \tag{7}$$

Fig. 5 Resistance as function of applied pressure for carbon nanotube network B1 for a fixed overlap length of 1.0 cm. Total resistance and NN1–NN2 contact resistance values are indicated by squares and circles, respectively. The line is a fit to eqn (7).
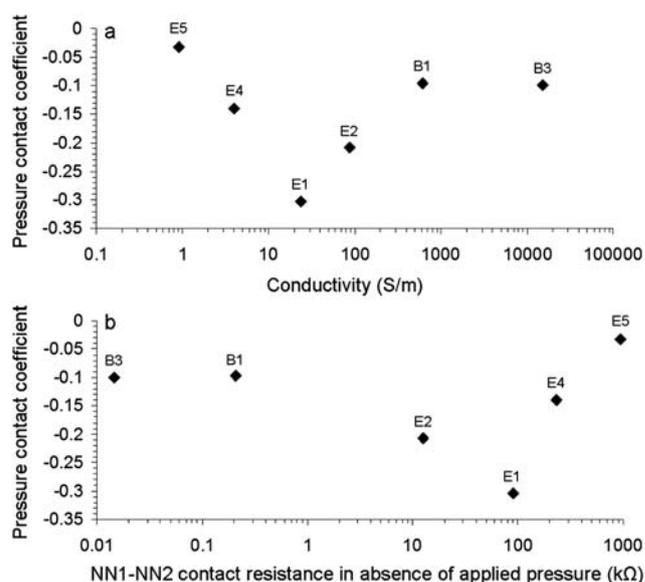

Fig. 6 Pressure coefficient as a function of (a) overall conductivity (σ_{ov}) and (b) NN1–NN2 contact resistance in the absence of applied pressure (R_{120}) for selected carbon nanotube networks. E1, E2, E4, E5, B1 and B3 refer to NN compositions as listed in Table 1.

where t is the power law exponent and R_{120} is the resistance at $P = 1 \text{ N m}^{-2}$, which happens to be equal to the pressure exerted on the overlap area due to the mass of the overlying NN on the underlying NN.

R_{120} and t are hereafter referred to as the NN1–NN2 contact resistance in the absence of applied pressure and the pressure coefficient, respectively. The latter is indicative of the dependence of inter-NN contact on pressure (see Table 2).

Fig. 6 shows that t is not an inherent NN parameter, *i.e.* it does not scale with the conductivity. Nevertheless, it does provide us with an insight into the connectivity between the overlapping NNs. Low t values are observed for those samples (E4, E5, B1 and B3) exhibiting low and high R_{120} values. This indicates that increasing pressure does not result in improvement of the conductivity. The reasons behind this similar behaviour are different. Low R_{120} values, as observed for samples B1 and B3 ($R_{120} < 0.2 \text{ k}\Omega$), indicate that there is already good connectivity between the overlapping NNs. Hence, increasing the pressure does little to improve the number of conducting pathways. High resistance values, as observed for samples E4 and E5 ($R_{120} > 200$ kΩ), suggest that the contact between NN1 and NN2 is highly resistive as a result of a near complete coverage of the nanotubes with dispersant (see also Fig. 2) and increasing the applied pressure has little effect.

NNs with higher t values (E1 and E2) exhibited for resistances ranging from 10 to 200 kΩ displayed a larger dependence on the applied pressure. This is likely to be related to the degree of CNT coverage by the dispersant, *i.e.* applying more pressure to a network consisting of partially covered CNTs will result in an increase in the number of conducting pathways. These results indicate that in order to reduce R_{12} by 50% for E1 requires a 10-fold increase in applied pressure, whereas for B1 a 1100-fold increase is needed.

Conclusions

The conductivity behaviour of eight carbon nanotube networks prepared using evaporative casting and vacuum filtration of HiPCO SWNT and CVD MWNT dispersed in gellan gum, xanthan gum and Triton X-100 solutions has been investigated. Resistance measurements as a function of length showed that both conductivity and electrode–NN contact resistance are influenced by the NN connectivity. Paradoxically, contact resistance values for the three NNs (samples B1–B3) prepared by vacuum filtration suggested near perfect connectivity even though their conductivity values varied by almost two orders of magnitude. Hence, we inferred that it is not possible to establish a measure of connectivity through a comparison of σ and R_C.

It was demonstrated that evaluating the resistance of two overlapping NNs as a function of the overlap distance (under constant applied pressure) is a viable method for calculating the electrical conductivity of NNs. Furthermore, we showed that this method can be used to calculate the connectivity between overlapping NN as well as to analyse the effects of varying pressure on connectivity. Using this approach we were able to show that the connectivity (NN1–NN2 contact resistance at constant pressure) is inversely proportional with the NN conductivity and can be fitted to a power law with exponent -0.8031. This is surprising as it appears to apply to all our NN irrespective of their nanotube type, fabrication method and utilised dispersant.

Finally, it was shown that insights into the dependence of inter-NN contact on applied pressure could be obtained through resistance measurements as a function of applied pressure on two overlapping NNs at a constant overlap distance. The connectivity as a function of applied pressure for each of the eight different NNs could be fitted to a power law. In this instance, the power law exponent t did not scale with conductivity, but did provide us with insights into NN connectivity. Low t values were observed for samples with low (<0.2 kΩ) and high (>200 kΩ) NN–NN resistance.

These observations lead us to suggest that increasing pressure does little to improve conductivity if there is either already good connectivity or highly resistive contact between the overlapping NNs. Contrary, applying more pressure to NNs with higher t values observed for NN with mid-range connectivity values (10–200 kΩ) should result in an increase in the number of conducting pathways. This work contributes to characterisation and understanding of gel–carbon nanotube materials.

Acknowledgements

Notes and references

1 S. J. Tans, A. R. M. Verschueren and C. Dekker, *Nature*, 1998, **393**, 49–52.
2 D. Mann, A. Javey, J. Kong, Q. Wang and H. Dai, *Nano Lett.*, 2003, **3**, 1541–1544.
3 C. T. White and T. N. Todorov, *Nature*, 1999, **393**, 240–242.
4 M. in het Panhuis, *J. Mater. Chem.*, 2006, **16**, 3598–3605.
5 H. Z. Geng, K. K. Kim, K. P. So, Y. S. Lee, Y. Chang and Y. H. Lee, *J. Am. Chem. Soc.*, 2007, **129**, 7758–7759.
6 U. Dettlaff-Weglikowska, V. Skakalov, R. Graupner, S. H. Jhang, B. H. Kim, H. J. Lee, L. Ley, Y. W. Park, S. Berber, D. Tomanek and S. Roth, *J. Am. Chem. Soc.*, 2005, **127**, 5125–5131.
7 A. Javey, J. Guo, Q. Wang, M. Lundstrom and H. Dai, *Nature*, 2003, **424**, 654–657.
8 P. Avouris, Z. H. Chen and V. Perebeinos, *Nat. Nanotechnol.*, 2007, **2**, 605–615.
9 A. G. Rinzler, J. Liu, H. Dai, P. Nikolaev, C. B. Huffman, F. J. Rodriguez-Macias, P. J. Boul, A. H. Lu, D. Heymann, D. T. Colbert, R. S. Lee, J. E. Fischer, A. M. Rao, P. C. Eklund and R. E. Smalley, *Appl. Phys. A: Mater. Sci. Process.*, 1998, **67**, 29–37.
10 K. Kordas, T. Mustonen, G. Toth, H. Jantunen, C. Soldano, S. Talapatra, S. Kar, R. Vajtai and P. M. Ajayan, *Small*, 2006, **2**, 1021–1025.
11 W. R. Small and M. in het Panhuis, *Small*, 2007, **3**, 1500–1503.
12 N. Songmee, S. Daothong and P. Singjai, *J. Nanosci. Nanotechnol.*, 2008, **8**, 2522–2525.
13 E. S. Snow, J. P. Novak, P. M. Campbell and D. Park, *Appl. Phys. Lett.*, 2003, **82**, 2145–2147.
14 F. Frehill, J. G. Vos, S. Benrezzak, A. A. Koos, Z. Konya, M. G. Ruther, W. J. Blau, A. Fonseca, J. B. Nagy, L. P. Biro, A. I. Minett and M. in het Panhuis, *J. Am. Chem. Soc.*, 2002, **124**, 13694–13695.
15 P. N. Nirmalraj, P. E. Lyons, S. De, J. N. Coleman and J. J. Boland, *Nano Lett.*, 2009, **9**, 3890–3895.
16 M. in het Panhuis, S. Gowrisanker, D. J. Vanesko, C. A. Mire, H. Jia, H. Xie, R. H. Baughman, I. H. Musselman, B. E. Gnade, G. R. Dieckmann and R. K. Draper, *Small*, 2005, **1**, 820–823.
17 G. Gruner, *J. Mater. Chem.*, 2006, **16**, 3533–3539.
18 K. Bradley, J.-P. C. Gabriel and G. Gruner, *Nano Lett.*, 2003, **3**, 1353–1355.
19 L. Hu, D. S. Hecht and G. Gruner, *Nano Lett.*, 2004, **4**, 2513–2517.
20 F. M. Blighe, Y. R. Hernandez, W. J. Blau and J. N. Coleman, *Adv. Mater.*, 2007, **19**, 4443–4447.
21 C. J. Ferris and M. in het Panhuis, *Soft Matter*, 2009, **5**, 1466–1473.
22 J. A. Boge, L. J. Sweetman, M. in het Panhuis and S. F. Ralph, *J. Mater. Chem.*, 2009, **19**, 9131–9140.
23 C. J. Ferris and M. in het Panhuis, *Soft Matter*, 2009, **5**, 3430–3437.
24 R. Bandyopadhyaya, E. Nativ-Roth, O. Regev and R. Yerushalmi-Rozen, *Nano Lett.*, 2002, **2**, 25–27.
25 E. Polaczek, L. Stobinski, J. Mazurkiewicz, P. Tomasik, H. Koloczekand and H. M. Lin, *Polimery*, 2007, **52**, 34–38.
26 M. in het Panhuis, A. Heurtematte, W. R. Small and V. N. Paunov, *Soft Matter*, 2007, **3**, 840–843.
27 A. M. Fialho, L. M. Moreira, A. T. Granja, A. O. Popescu, K. Hoffman and I. Sa-Correia, *Appl. Microbiol. Biotechnol.*, 2008, **79**, 889–900.
28 L. D. L. Melton, D. A. Mindt and G. R. Sanderson, *Carbohydr. Res.*, 1976, **46**, 245–257.
29 P. E. Jansson, B. Lindberg and P. A. Sandford, *Carbohydr. Res.*, 1983, **124**, 135–139.
30 S. C. Kumar, C. S. Satish and H. G. Shivakumar, *J. Macromol. Sci., Part A: Pure Appl. Chem.*, 2008, **45**, 643–649.
31 A. M. Smith, R. M. Shelton, Y. Perrie and J. J. Harris, *J. Biomater. Appl.*, 2007, **22**, 241–254.
32 P. E. Lyons, S. De, F. M. Blighe, V. Nicolosi, L. F. C. Pereira, M. S. Ferreira and J. N. Coleman, *J. Appl. Phys.*, 2008, **104**, 044302.